demanded pump head was reserved by the modifications such as the attachment of the front shroud.

5.3 Anti-Hemolysis Performance

Figure 13 shows the wall shear stress of Prototype 2. The regions with the shear stress higher than 16Pa exist only on the casing wall near the inlet of the impellers, as shown in Figs.13(a) and (d). The area of the high wall shear stress in Prototype 2 is much smaller than the results shown in Fig.6 for Prototype 1. Therefore, it can be expected that Prototype 2 has a high anti-hemolysis performance.

5.4 Anti-Thrombosis Performance

Figure 14 shows the velocity vectors in the return channel of Prototype 2, which are the velocity vectors on the cross-section D'-D' shown in Fig.8. The stagnation does not appear in the return channel. Figure 15 shows the flow field in a meridian cross-section. The enlarged view of the clearance between the backshroud of the 1st impeller and the shroud of the return channel is shown in the left side of Fig.15. In the enlarged view, the fluid near the backshroud of the 1st impeller flows radially outward and the fluid near the shroud of the return channel flows radially inward. However, the velocity V/U_t in the clearance is as small as from about 0 to 0.1 and the possibility of the thrombosis cannot be denied. On the other hand, the velocity V/U_t in the clearance between the backshroud of the 2nd impeller and the casing is as large as from about 0.1 to 0.5. There is a part which is better to be

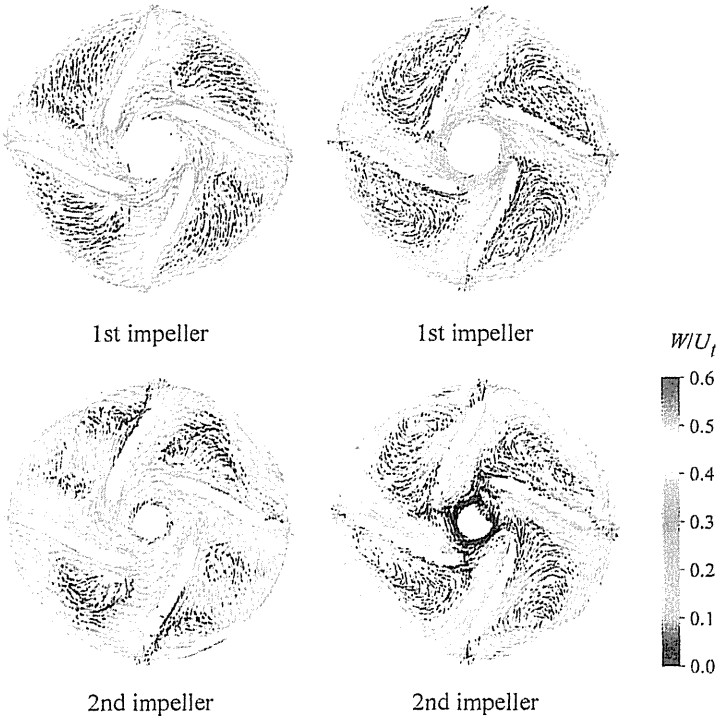

(a) Original (Prototype1) (b) Impeller with front shroud

Fig. 10 Velocity vector near the back shroud in the original and modified impellers of Prototype 1 at $Q=Q_d$

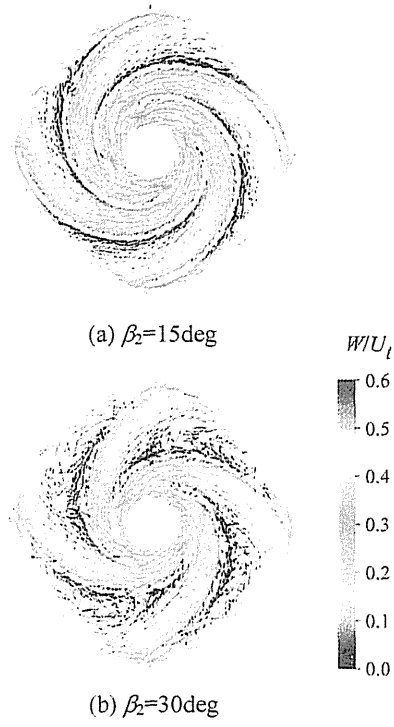

Fig. 11 Velocity vector near the back shroud of 1st impellers with β_2=15deg and 30deg. The impellers have front shroud and the 2nd impeller has four washout holes. $Q=Q_d$ and N=1200rpm. SST turbulence model was used.

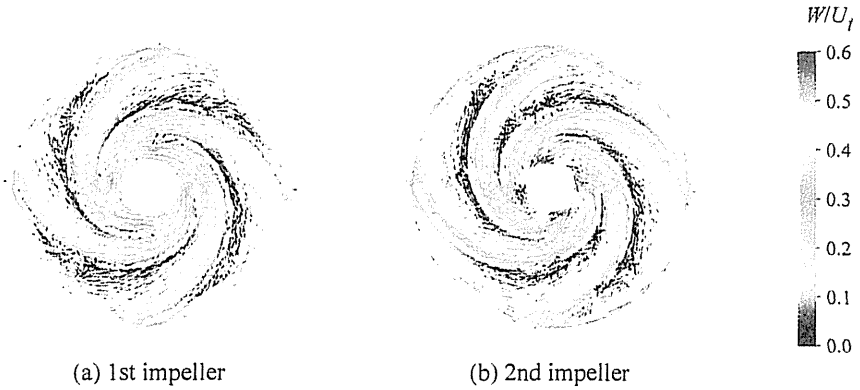

(a) 1st impeller (b) 2nd impeller

Fig. 12 Velocity vector near the back shroud of impellers with β_2=20deg in Prototype 2 at $Q=Q_d$ and N=1200rpm. SST turbulence model was used.

still improved, but better flow fields are achieved in Prototype 2, compared to the flow fields of Prototype 1.

5.5 Anti-Hemolysis and Thrombosis Performances at Off-Design Operating Conditions

The wall shear stress around the tongue at Q=1.63Q_d is shown in Fig.16. Q=1.63Q_d with the water at N=1150rpm corresponds to Q=5L/min with the blood at N=4000rpm. The region with the shear stress higher than 16Pa can be observed and it is thought to be caused by the increase of the flow velocity. The shear stresses on the walls except around the tongue were similar to those at Q=Q_d and the flows in the impellers and the return channel were smoother than those at Q=Q_d. The velocity vector near the back shroud of 1st impeller at Q=0.33Q_d is shown in Fig.17. Q=0.33Q_d with the water at N=1150rpm corresponds to Q=1L/min with the blood at N=4000rpm. The flow separation can be observed over a wide region of the pressure surface of the blades in Fig.17. As the flow velocities are small due to the low flow rate, the operations with the low flow rate have a possibility of the occurrence of the thrombosis in the stagnation caused by the flow separation. The flow separations were also observed in the 2nd impeller and the return channel. The wall shear stresses at Q=0.33Q_d were similar to those at Q=Q_d. Therefore, in the operations of Prototype 2, it is necessary to pay attention to the occurrence of the hemolysis at higher flow rates and the thrombosis at lower flow rates.

5.6 Pump Performance

The pump performance of Prototype 2 is shown in Fig.18. The horizontal axis shows the flow rate and the vertical axis shows the pump head. The experiment was conducted using the water at ordinary temperatures in the rotational speed of 1150rpm.

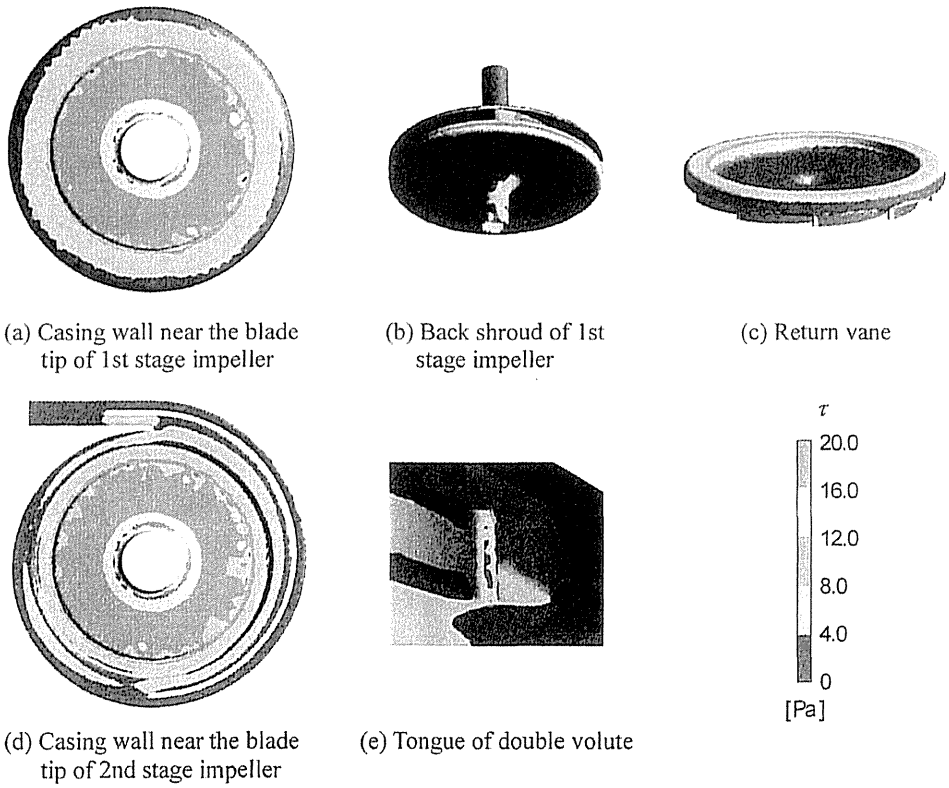

(a) Casing wall near the blade tip of 1st stage impeller

(b) Back shroud of 1st stage impeller

(c) Return vane

(d) Casing wall near the blade tip of 2nd stage impeller

(e) Tongue of double volute

Fig. 13 Wall shear stress distribution on Prototype 2 at Q=Q_d. N=1150 rpm

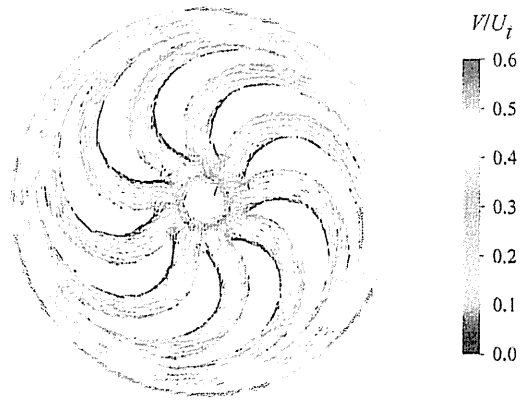

Fig. 14 Velocity vector on the cross-section (D'-D' in Fig.8) of the return channel in Prototype 2 at Q=Q_d. N=1150rpm

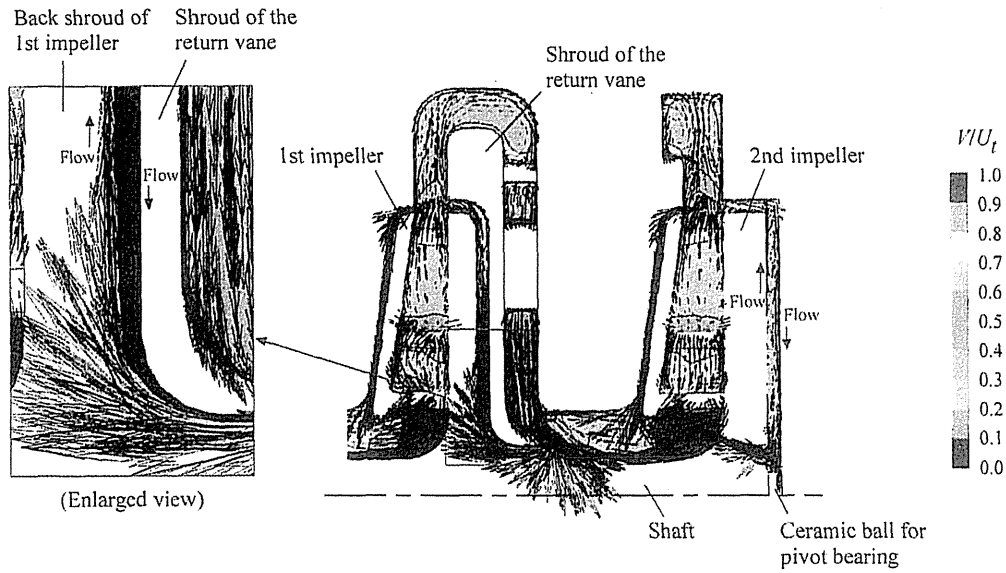

Fig. 15 Flow field on the meridian plane of Prototype 2 at $Q=Q_d$. N=1150rpm

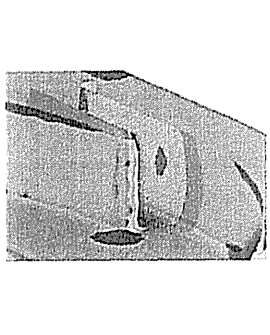

Fig. 16 Wall shear stress around the tongue of double volute of Prototype 2 at Q=1.63Q_d and N=1150rpm, which correspond to Q=5L/min and N=4000rpm with the blood

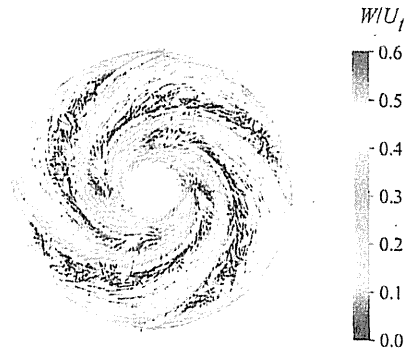

Fig. 17 Velocity vector near the back shroud of 1st impeller in Prototype 2 at Q=0.33Q_d and N=1150rpm, which correspond to Q=1L/min and N=4000rpm with the blood

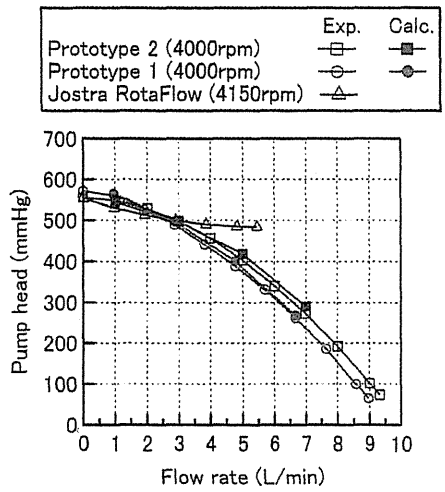

Fig. 18 Pump performance

Considering an easy understanding in clinical practice, the results were converted into the values in the operation with the blood at 4000 rpm, using the relation of $\Delta p_{blood} = \Delta p_{water} \cdot \rho_{blood} \cdot U_{t,blood}^2 / (\rho_{water} \cdot U_{t,water}^2)$. The pump performance of Prototype 1 is also plotted. The demanded pump performance of 500mmHg at 3L/min can be obtained and the performance curve is similar to that of Prototype 1. The pump performance of the Jostra RotaFlow centrifugal pump is also shown in Fig.18. The results was obtained through translating the results at 1200rpm with the water into the results at 4150rpm with the blood. The slope of the performance curve of Prototype 2 is steeper than that of the Jostra RotaFlow centrifugal pump in usable ranges of 1-5L/min, as in the case of Prototype 1. This indicates that the flow rate is insensitive to the flow resistance. This is an advantage because the stable flow rate can be kept easier. The computational results for Prototype 1 and 2 are shown in Fig.18. The computational results agree with the experimental results well.

The measurement of the efficiency except the torque due to the pivot bearings was conducted, but the stable values of the efficiency could not be obtained because the torque due to the friction in the pivot bearing was not stable in the operation with the air. This seems to be caused by the occurrence of the thrust load due to the decrease of the axial fluid force when the air is used as the working fluid. The efficiency which includes the friction loss of the pivot bearing was about 12% at $Q=Q_d$ and the maximum efficiency was about 15% at 5L/min.

5.7 Pressure Distribution

The pressure distributions in Prototype 1 and 2 are shown in Figs.19(a) and (b), respectively. The pressure was measured at the measuring points shown in Figs.5 and 9. In the case of Prototype 1, the flow rates were set to 0.29, 0.86, 1.44, 2.01, 2.57L/min at 1200rpm. These flow rates correspond to 1.0, 2.9, 4.8, 6.7, 8.6L/min at the operation of 4000rpm using the blood as the working fluid. In the case of Prototype 2, the flow rates were set to 0.29, 0.86, 1.44, 2.01L/min at 1150rpm. These flow rates correspond to 1.0, 3.0, 5.0, 7.0L/min at the operation of 4000rpm using the blood. In both cases, the results are converted into the values in the operation with the blood at 4000rpm. The horizontal axis represents the measuring point and the vertical axis represents the

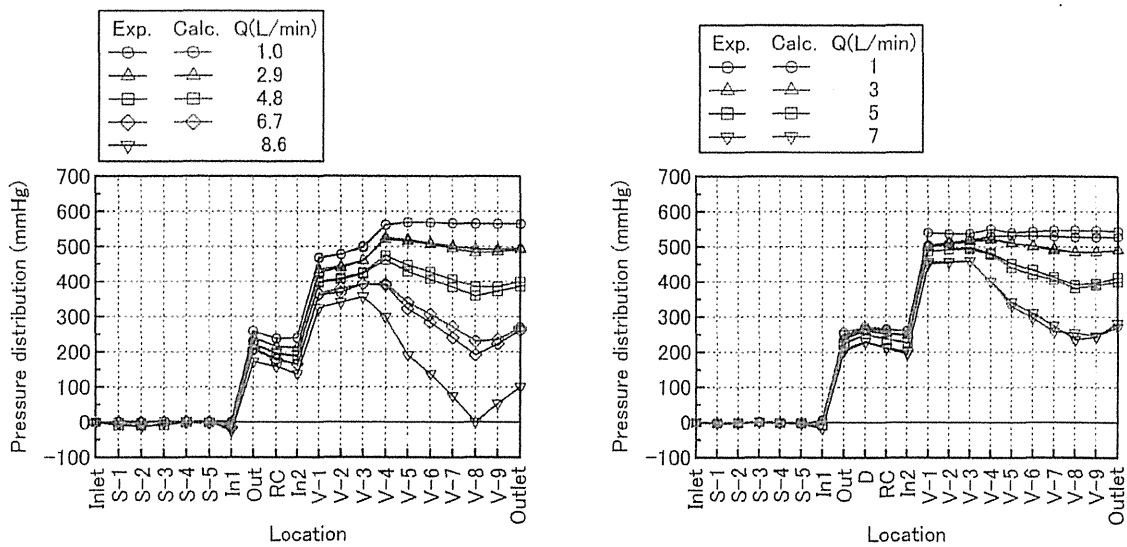

(a) Prototype 1 (b) Prototype 2

Fig. 19 Pressure distributions in the pumps

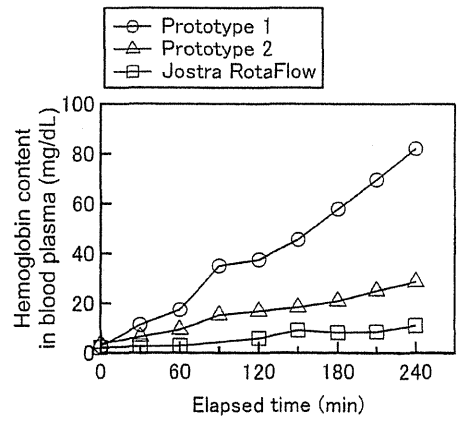

Fig. 20 Result of the hemolysis test with fresh goat blood at $Q=Q_d$ (3L/min) and $H=H_d$ (500mmHg)

difference of the pressure at the measuring point from the pressure at the inlet. The values at In1, Out, RC, In2 are the circumferentially averaged values. The experimental and computational results are shown by black and red colors, respectively.

The computational results are in good agreement with the experimental results. It was found that the work done by the 1st impeller (In1-Out) was almost the same as the work done by the 2nd impeller (In2-V-1) in both pumps of Prototype 1 and 2, as shown in Figs.19(a) and (b). It was also found that the pressure at the outlet (V-1) of the 2nd impeller in Prototype 2 was higher than that in Prototype 1 and the amount of the pressure recovery in the volute casing of Prototype 2 was not more than that in Prototype 1.

5.8 Hemolysis Test

The result of the hemolysis test is shown in Fig.20. The result is for the case that the flow rate and the pump head are the design values of 3L/min and 500mmHg, respectively. The horizontal axis represents the elapsed time and the vertical axis represents the hemoglobin content in the blood plasma. The rotational speeds of Prototype 1, 2, and the Jostra RotaFlow centrifugal pump were 4010rpm, 3980rpm, and 4240rpm, respectively. The amount of the hemolysis in Prototype 2 is as small as about one third of that in Prototype 1 after a lapse of four hours (240min). This shows that the design aimed at the decrease of the wall shear stress is effective for the decrease of the amount of the hemolysis.

As shown in Fig.20, the amounts of the hemolysis of Prototype 1 and 2 were larger than that of the Jostra RotaFlow centrifugal pump. In addition to further decrease of the wall shear stress, the design method considering the exposure time of the blood to a shear flow may be necessary because the exposure time is considered to affect the amount of the hemolysis [7, 8]. In the present study, it was also found that the hemolysis occurred at the high pump head of 500mmHg (at the high rotational speed) in the Jostra RotaFlow centrifugal pump, which is considered to have a high anti-hemolysis performance at lower pump heads (at lower rotational speeds). The realization of blood pumps with higher anti-hemolysis performance is desired.

5. Conclusions

The improvement of a prototype of two-stage centrifugal blood pump for the cardiopulmonary support system was conducted and the hemolysis test for the first prototype and the improved pump was performed. The results obtained in the present study are summarized as follows.

(1) Due to the attachment of the front shroud to the impeller, vortices which could cause the thrombosis occurred in the impeller. The occurrence of the vortices could be prevented by the change of the outlet blade angle of the impeller.

(2) The front shroud of the impeller was effective for the decrease of the wall shear stress on the casing near the tip of the impeller.

(3) The movement of the leading edge of the return guide vane and the tongue of the double volute casing away from the outlet of the impeller led to the decrease of the circumferential velocity around them and was effective to the decrease of the shear stress on them.

(4) The design method of the return guide vane which covered the region of the flow separation was effective for the suppression of the stagnation. The increase of the number of the vanes which led to the decrease of the region of the flow separation and the vane thickness was also effective for giving an uniform radial flow at the outlet of the return channel.

(5) The slope of the performance curve of the improved pump was as large as that of the first prototype. This is an advantage because the flow rate is insensitive to the change of the flow resistance. In the comparison of the pressure distributions, it was confirmed that the computational results agreed well with the experimental results.

(6) The amount of the hemolysis in the improved pump was about one third of that in the first prototype. This indicates that the decrease of the wall shear stress is effective for improving the anti-hemolysis performance of blood pumps.

Acknowledgments

The present study was supported by JSPS Grant-in-Aid for Scientific Research (B) (Grant Number 18360094 and 20360091 Principal Investigator: Dr. Tomonori Tsukiya).

Nomenclature

C	Tip clearance	Δp	Pressure difference
D_t	Diameter of impeller	μ	Viscosity
h	Blade height	ν	Kinetic viscosity
H	Pump head	ρ	Fluid density
N	Rotational speed	τ	Shear stress
Q	Volumetric flow rate	**Subscript**	
Re	Reynolds number ($=U_tD_t/\nu$)	1	Inlet
U_t	Tip speed of impeller	2	Outlet
V	Absolute velocity	*blood*	Blood
W	Relative velocity	*d*	Reference
β	Blade angle	*water*	Water

References

[1] Horiguchi, H, Tsukiya, T., Nomoto, T., Takemika, T., and Tsujimoto, Y., 2014, "Study on the Development of Two-Stage

Centrifugal Blood Pump for Cardiopulmonary Support System," International Journal of Fluid Machinery and Systems, Vol. 7, No. 4, pp.142-150. (DOI: 10.5293/IJFMS.2014.7.4.142)
[2] ANSYS, Inc., 2006, "Modeling Flow Near the Wall", ANSYS CFX-Solver Modeling Guide, Release 11, pp.125-127.
[3] ANSYS, Inc., 2006, "Modeling Flow Near the Wall", ANSYS CFX-Solver Theory Guide, Release 11, pp.110-111.
[4] Takeda, H., 2005, "Basic Design on Pumps (in Japanese)," Dengyosha Technical Review, Vol. 29, No. 2, pp. 7-14. (http://www.dmw.co.jp/technical/pdf/no57.pdf)
[5] Kameneva, M. V., Burgreen, G. W., Kono, K., Repko, B., Antaki, J. F., and Umezu, M., 2004, "Effects of Turbulent Stresses upon Mechanical Hemolysis: Experimental and Computational Analysis," ASAIO Journal, Vol. 50, No. 5, pp. 418-423.
[6] Stepanoff, A. J., 1957, "Centrifugal and Axial Flow Pumps (Second Edition)," John Wiley & Sons Inc., pp. 172.
[7] Heuser, G., Opitz, R., 1980, "A Couette Viscometer for Short Time Shearing of Blood," Biorheology, Vol. 17, pp. 17-24.
[8] Giersiepen, M., Wurzinger, L. J., Opitz, R., and Reul, H., 1990, "Estimation of Shear Stress-Related Blood Damage in Heart Valve Prostheses – in Vitro Comparison of 25 Aortic Valves," The International Journal of Artificial Organs, Vol. 13, No. 5, pp. 300-306.

J Artif Organs (2015) 18:35–39
DOI 10.1007/s10047-014-0804-y

ORIGINAL ARTICLE

Cardiopulmonary Bypass

A novel small animal extracorporeal circulation model for studying pathophysiology of cardiopulmonary bypass

Yutaka Fujii · Mikiyasu Shirai · Shuji Inamori · Yoshiaki Takewa · Eisuke Tatsumi

Received: 23 May 2014 / Accepted: 21 October 2014 / Published online: 6 November 2014

Abstract Extracorporeal circulation (ECC) is indispensable for cardiac surgery. Despite the fact that ECCcauses damage to blood components and is non-physiologic, its pathophysiology has not been fully elucidated. This is because difficulty in clinical research and animal experiments keeps the knowledge insufficient. Therefore, it is desirable to have a miniature ECC model for small animals, which enables repetitive experiments, to study the mechanism of pathophysiological changes during ECC. We developed a miniature ECC system and applied it to the rat. We measured changes in hemodynamics, blood gases and hemoglobin (Hb) concentration, serum cytokines (TNF-α, IL-6, IL-10), biochemical markers (LDH, AST, ALT), and the wet-to-dry weight (W/D) ratio of the lung for assessing whether the rat ECC model is comparable to the human ECC. The ECC system consisted of a membranous oxygenator (polypropylene, 0.03 m^2), tubing line (polyvinyl chloride), and roller pump. Priming volume of this system is only 8 ml. Rats (400–450 g) were divided into the SHAM group ($n = 7$) and the ECC group ($n = 7$). Blood samples were collected before, 60 and 120 min after initiation of ECC. During ECC, blood pressure and Hb were maintained around 80 mmHg and 10 g/dL, respectively. The levels of the inflammatory and biochemical markers and the W/D ratio were significantly elevated in the ECC group, indicating some organ damages and systemic inflammatory responses during ECC. We successfully established the ECC for the rat. This miniature ECC model could be a useful approach for studying the mechanism of pathophysiology during ECC and basic assessment of the ECC devices.

Keywords Extracorporeal circulation · Rat ECC model · Inflammatory response · Biological reaction

Y. Fujii (✉) · Y. Takewa · E. Tatsumi
Department of Artificial Organs, National Cerebral and Cardiovascular Center Research Institute, 5-7-1, Fujishiro-dai, Suita, Osaka 565-8565, Japan
e-mail: yfujii@ncvc.go.jp

M. Shirai
Department of Cardiac Physiology, National Cerebral and Cardiovascular Center Research Institute, 5-7-1, Fujishiro-dai, Suita, Osaka 565-8565, Japan

S. Inamori
Department of Clinical Engineering Faculty of Health Sciences, Hiroshima International University, 555-36, Kurose-gakuendai, Higashi-hiroshima, Hiroshima 739-2631, Japan

Introduction

Extracorporeal life support (ECLS) devices, such as the cardiopulmonary bypass, preserve the patient's life by providing adequate oxygen supply and blood flow to vital organs [1]. However, cardiac surgery with the use of extracorporeal circulation (ECC) is often accompanied by the systemic inflammatory response, influencing significantly the morbidity and mortality after ECC [2]. Further studies are needed to elucidate the pathophysiology during ECC. However, difficulty in clinical research and animal experiments keeps its elucidation insufficient. Therefore, it is desirable to have a miniature ECC model for small animals, which enables repetitive experiments, to study the mechanism of pathophysiological changes during artificial perfusion.

In this study, we developed a miniature ECC model and applied the system to the rat. For assessing whether the rat ECC model is comparable to the human ECC, we measured changes in the hemodynamics, blood gases and Hb,

serum cytokines: tumor necrosis factor-α (TNF-α), interleukin-6 (IL-6), and interleukin-10 (IL-10), and biochemical markers: lactate dehydrogenase (LDH), aspartate aminotransferase (AST), and alanine aminotransferase (ALT), and the wet-to-dry weight (W/D) ratio of the lung.

Materials and methods

Animal

The study was approved by the National Cerebral and Cardiovascular Center Research Institute Animal Care and Use Committee, and all procedures met the National Institutes of Health guidelines for animal care.

Sprague–Dawley rats (male 400–450 g) were housed three per cage under a 12-h light–dark cycle with food and water available ad libitum.

Anesthesia, surgical preparation, and extracorporeal circulation

The animals were anesthetized with pentobarbital sodium (50 mg/kg body weight intraperitoneal injection), placed in the supine position and rectal thermocouple probe kept in place. Then, orotracheal intubation was performed using a 14G cannula (Insyte BD Medical, Sandy, Utah) and rats were ventilated with a respirator (Model SN-480-7, Shinano Seisakusho Co., Ltd, Tokyo, Japan). Ventilation was volume-controlled at a frequency of 70/min, a tidal volume of 8–10 ml/kg body weight and 100 % of inspired oxygen fraction. Rectal temperature was maintained at 36 °C throughout the experiment. Arterial blood pressure was monitored (Model 870, PowerLab system, AD Instruments, Castle Hill, Australia) via the femoral artery, which was cannulated with polyethylene tubing (SP-31 Natsume Seisakusho Co., Ltd, Tokyo, Japan). The left common carotid artery was cannulated with a polyethylene tubing (SP-55 Natsume Seisakusho Co., Ltd, Tokyo, Japan) to serve as the arterial inflow cannula for the ECC circuit. 500 IU/kg heparin sodium was administered after placement of this cannula. A 16G cannula (Insyte BD Medical, Sandy, Utah) was advanced through the right external jugular vein into the right atrium and served as a conduit for venous outflow.

The small animal ECC system (Fig. 1) consisted of a membranous oxygenator (polypropylene, 0.03 m^2: Senko Medical Co., Ltd, Osaka, Japan), tubing line (Senko Medical Co., Ltd, Osaka, Japan) and roller pump (Micro tube pump MP-3 Tokyo Rikakikai Co., Ltd, Tokyo, Japan) was primed by 5 ml of Ringer's solution, 1 ml of mannitol, 1 ml of sodium bicarbonate, and 1 ml (1000 IU) of heparin. Total priming volume of this system was 8 ml.

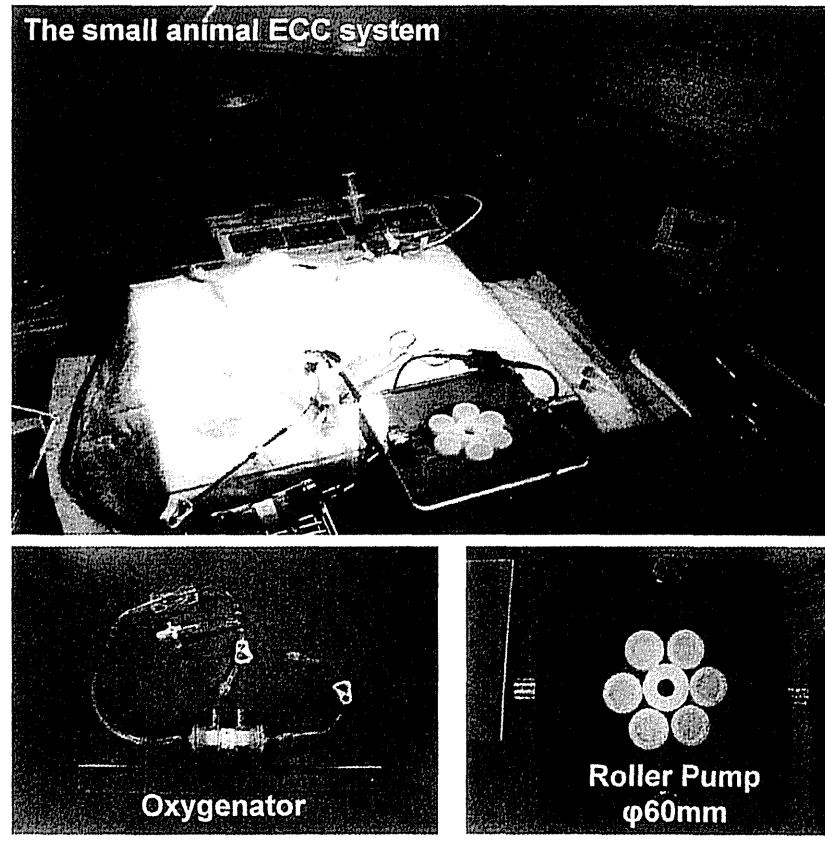

Fig. 1 The small animal ECC system. Polypropylene membranous oxygenator with membrane area of 0.03 m^2 and polyvinyl chloride tubing line (Senko Medical Co., Ltd, Osaka, Japan), and roller pump (MP-3 Tokyo Rikakikai Co., Ltd, Tokyo, Japan) are shown

Experimental design

The animals were divided into 2 groups: SHAM group ($n = 7$) and ECC group ($n = 7$). The SHAM group received surgical preparation only without CPB. In the ECC group, ECC was initiated and maintained at 70 ml/kg/min for 60 min.

Partial pressure of arterial carbon dioxide ($PaCO_2$) and partial pressure of arterial oxygen (PaO_2) were maintained at 35–45 mmHg and 300–400 mmHg. Blood samples were collected at three defined time points, before ECC (pre-ECC), 60 min after initiation of ECC. and 120 min after initiation of ECC (end-ECC).

To evaluate the inflammatory responses [3], TNF-α, IL-6, IL-10 were measured by enzyme-linked immunosorbent assay (ELISA kit, R&D systems, MN, USA). The concentrations of LDH, AST, and ALT which are used as biochemical markers for evaluating organ damage [4] were measured (DRI-CHEM 7000 Analyzer, FUJIFILM, Kanagawa, Japan).

Blood gases, pH, hemoglobin concentration, and electrolytes were also measured (ABL800 FLEX system, RADIOMETER, Copenhagen, Danmark). Animals in which the hemoglobin level declined to less than 8 g/dL at any point were excluded from the study. In general, when the hemoglobin becames 7–8 g/dL in clinical site, we consider blood transfusion [5, 6]. In this study, the purpose was to perform extracorporeal circulation without blood transfusion. All animals were killed at the end of ECC by potassium chloride injection and the left lung was harvested and divided into three parts. The superior third was used for the calculation of W/D ratio. The lung block was weighed before and after desiccation for 72 h in a dry oven at 70 °C.

Statistics

All data are expressed as mean ± standard deviation (SD). The Student's t test was used for subsequent comparison between groups at the same time points. All statistical analyses were performed using Stat-View 5.0 (Abacus Concepts, Berkeley, CA). Significance was set at $P < 0.05$.

Results

Table 1 shows the changes in hemodynamic variables, Hb concentration, PaO_2, $PaCO_2$, and level of electrolyte in the SHAM and ECC groups during experiments. During ECC, MAP and Hb were significantly decreased but were maintained around 80 mmHg and 10 g/dL, respectively. All rats' hemoglobin level did not fall below 8 g/dL at any point. There was no exclusion in the both groups. There were no significant changes in the value of the electrolyte in the both groups. However, in the ECC group, it tended to high potassium during ECC.

Table 1 Hemodynamic variables, Hb and blood gas partial pressures, and level of electrolyte before and during ECC

	Group	Pre-ECC	ECC 60 min	ECC 120 min
MAP (mmHg)	SHAM	103 ± 11	100 ± 13	105 ± 11
	ECC	102 ± 5	94 ± 24	87 ± 19*
HR (beat/min)	SHAM	387 ± 38	373 ± 38	389 ± 26
	ECC	395 ± 25	366 ± 30	365 ± 17
PaO_2 (mmHg)	SHAM	110 ± 17	106 ± 16	105 ± 14
	ECC	112 ± 12	421 ± 40*	412 ± 34*
$PaCO_2$ (mmHg)	SHAM	38 ± 3	37 ± 2	40 ± 2
	ECC	41 ± 3	40 ± 3	39 ± 3
Hb (mg/dL)	SHAM	14.7 ± 1.1	14.5 ± 0.9	14.2 ± 0.9
	ECC	15.1 ± 1.0	11.8 ± 1.1*	11.6 ± 1.0*
Na (mEq/L)	SHAM	139.6 ± 1.1	140.6 ± 1.2	141.0 ± 0.9
	ECC	138.9 ± 0.9	141.2 ± 1.0	142.0 ± 1.3
K (mEq/L)	SHAM	5.2 ± 0.2	5.4 ± 0.3	5.5 ± 0.3
	ECC	5.1 ± 0.2	5.7 ± 0.4	5.9 ± 0.5
Cl (mEq/L)	SHAM	105.6 ± 1.5	108.6 ± 1.4	107.3 ± 2.1
	ECC	106.1 ± 1.8	108.9 ± 2.2	108.7 ± 2.7

Variables are expressed by mean ± standard deviation

* $P < 0.05$ versus SHAM group at the same time

Before ECC, the serum levels of inflammatory and biochemical markers were not statistical different between the SHAM and ECC groups. Serum inflammatory and biochemical markers remained unchanged during experiment periods in the SHAM group. In the ECC group, all the systemic inflammatory markers increased significantly, reaching a maximum (TNF-α 1129 ± 137 pg/ml, IL-6 1157 ± 150 pg/ml, IL-10 385 ± 55 pg/ml) at the end of ECC (Fig. 2a–c). Additionally, in the ECC group, the levels of biochemical markers significantly increased (LDH 425 ± 65 U/L, AST 113 ± 6 U/L, ALT 55 ± 8 U/L) 60 min after the ECC initiation and increased further (LDH 708 ± 126 U/L, AST 76 ± 7 U/L, ALT 159 ± 14 U/L) 120 min after the ECC initiation (Fig. 2d–f).

The ECC group showed significantly higher W/D ratio of the lung than the SHAM group (SHAM 4.68 ± 0.18, ECC 5.46 ± 0.23) (Fig. 3).

Discussion

In this study, our small animal ECC system was able to maintain adequate levels of blood gases and Hb, and blood pressure. Furthermore, our model offers the advantage of a low priming volume not requiring transfusion in ECC group rats.

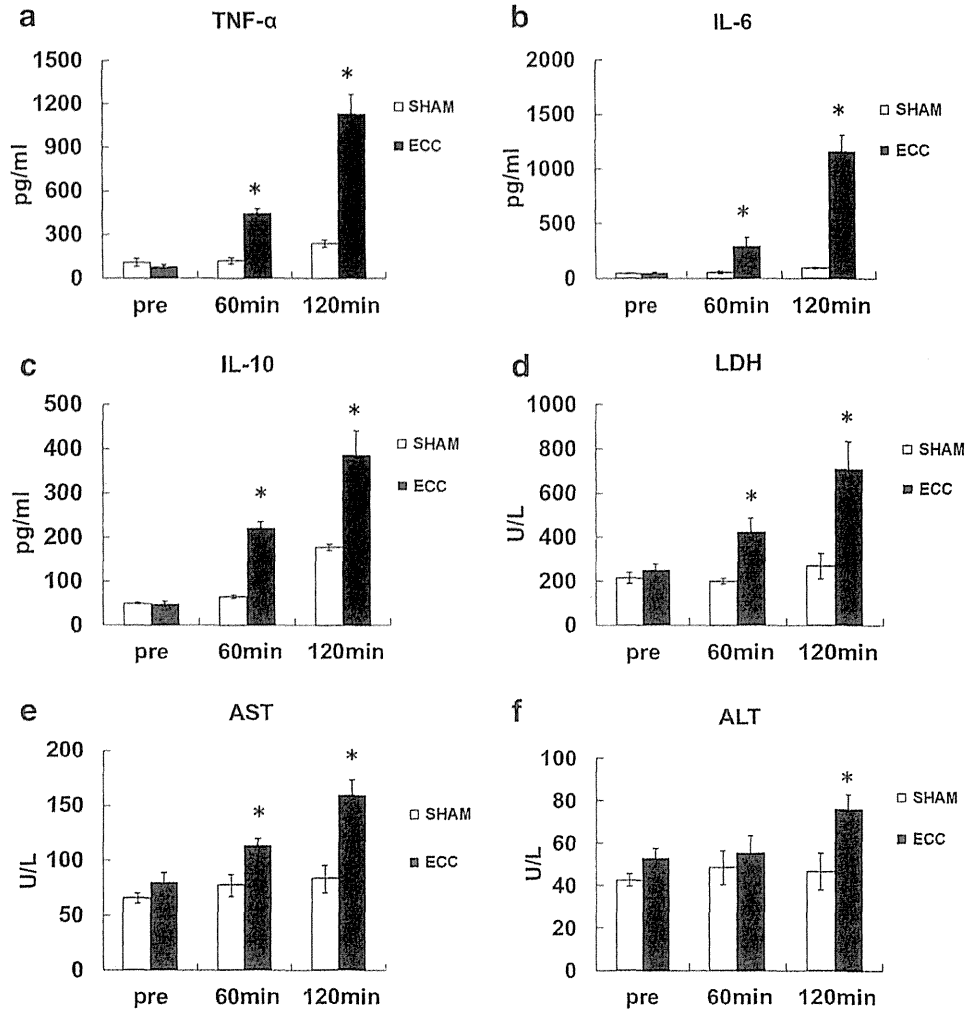

Fig. 2 Serum tumor necrosis factor (TNF)-α (**a**), interleukin (IL)-6 (**b**), interleukin (IL)-10 (**c**), lactate dehydrogenase (LDH) (**d**), aspartate aminotransferase (AST) (**e**), alanine aminotransferase (ALT) (**f**). *$P < 0.05$ versus SHAM group at the same time periods

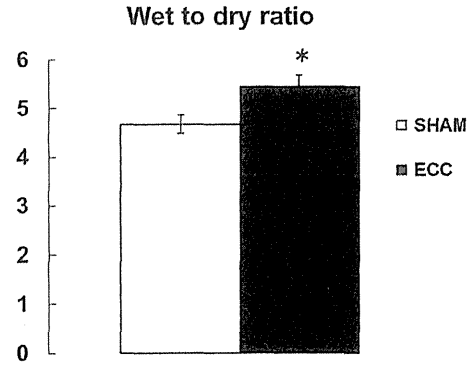

Fig. 3 Wet-to-dry ratio of the left lung at the end of CPB. *$P < 0.05$ versus SHAM group

The significant systemic inflammatory responses occurred, reaching a maximum at the end of ECC. Additionally, the biochemical markers reflecting organ damages significantly increased 60 min after the ECC initiation and increased further 120 min after the ECC initiation. The significant increase in the W/D ratio of the lung which suggests pulmonary edema [7, 8] is consistent with the previous study data [9]. From these data, our rat ECC model is considered useful for studying mechanism of pathophysiology during ECC, as an alternative to the established human ECC, which is often associated with systemic inflammation and organ damage [10].

It has been suggested that the factors responsible for the inflammatory response during ECC are blood contact with the surface of the extracorporeal circulation unit, endotoxemia, surgical trauma, ischemic reperfusion injury, and blood loss [10, 11]. Many studies showed the blood contacting surface of the ECC circuit activates white cells, platelets, and the complement system. The increase in cytokines, such as interleukins and necrosis factor [12], aggravates the inflammatory response [13]. These complex interactions during ECC lead to further inflammation [13]. In our rat ECC models, the insufflation of hydrogen which selectively reduces the hydroxyl radical could decrease the levels of serum cytokines and biochemical markers, and the

W/D ratio of the lung [7, 8]. These findings suggest that hydroxyl radical contributes toward promoting the systemic inflammatory responses and organ damages during ECC [7, 8].

In the current study, we have not been able to perform an analysis of hemolysis. The possibility of hemolysis in the ECC group cannot be denied. Therefore, in the next study, we are going to analyze for damage of blood cells. Furthermore, in the future, we will conduct research on pathophysiology of cardiopulmonary bypass by using this novel small ECC model.

Conclusion

In this study, we developed a novel small ECC model and applied the system to the rat. In our rat ECC models, we demonstrated that adequate levels of blood gases and Hb, and blood pressure were maintained and that the systemic inflammatory response and organ damages including pulmonary edema were induced associated with the production of cytokines. This novel small ECC model could be a useful approach for studying the mechanism of pathophysiology (systemic inflammation and organ damage) during ECC and basic assessment of the ECC devices.

Conflict of interest The authors have no conflict of interest directly relevant to the content of this article.

References

1. Walker G, Liddell M, Davis C. Extracorporeal life support-state of the art. Paediatr Respir Rev. 2003;4:147–52.
2. Gao D, Grunwald GK, Rumsfeld JS, Mackenzie T, Grover FL, Perlin JB, McDonald GO, Shroyer AL. Variation in mortality risk factors with time after coronary artery bypass graft operation. Ann Thorac Surg. 2003;75:74–81.
3. Pasquale MD, Cipolle MD, Monaco J, Simon N. Early inflammatory response correlates with the severity of injury. Crit Care Med. 1996;24:1238–42.
4. Jiang Hongchi, Meng Fanqiang, Li Wei, Tong Liquan, Qiao Haiquan, Sun Xueying. Splenectomy ameliorates acute multiple organ damage induced by liver warm ischemia reperfusion in rats. Surgery. 2007;141:32–40.
5. Developed by the Task Force on Blood Component Therapy. Practice guidelines for blood component therapy: a report by the American Society of Anesthesiologists Task Force on blood component therapy. Anesthesiology. 1996;84:732–47.
6. de Gast-Bakker DH, de Wilde RB, Hazekamp MG, Sojak V, Zwaginga JJ, Wolterbeek R, de Jonge E, Gesink-van der Veer BJ. Safety and effects of two red blood cell transfusion strategies in pediatric cardiac surgery patients: a randomized controlled trial. Intensiv Care Med. 2013;39:2011–9.
7. Fujii Y, Shirai M, Inamori S, Shimouchi A, Sonobe T, Tsuchimochi H, Pearson JT, Takewa Y, Tatsumi E, Taenaka Y. Insufflation of hydrogen gas restrains the inflammatory response of cardiopulmonary bypass in a rat model. Artif Organs. 2013;37:136–41.
8. Fujii Y, Shirai M, Tsuchimochi H, Pearson JT, Takewa Y, Tatsumi E, Taenaka Y. Hyperoxic condition promotes an inflammatory response during cardiopulmonary bypass in a rat model. Artif Organs. 2013;37:1034–40.
9. Aebert H, Kirchner S, Keyser A, Birnbaum DE, Holler E, Andreesen R, Eissner G. Endothelial apoptosis is induced by serum of patients after cardiopulmonary bypass. Eur J Cardiothorac Surg. 2000;18:589–93.
10. Boyle EM, Pohlman TH, Johnson MC, Verrier ED. Endothelial cell injury in cardiovascular surgery: the systemic inflammatory response. Ann Thorac Surg. 1997;63:277–84.
11. Butler J, Rocker GM, Westaby S. Inflammatory response to cardiopulmonary bypass. Ann Thorac Surg. 1993;55:552–9.
12. Engelman RM, Rousou JA, Flack JE 3rd, Deaton DW, Kalfin R, Das DK. Influence of steroids on complement and cytokine generation after cardiopulmonary bypass. Ann Thorac Surg. 1995;60:801–4.
13. Cremer J, Martin M, Redl H, Bahrami S, Abraham C, Graeter T, Haverich A, Schlag G, Borst HG. Systemic inflammatory response syndrome after cardiac operations. Ann Thorac Surg. 1996;61:1714–20.

Investigation of the biological effects of artificial perfusion using rat extracorporeal circulation model

Yutaka Fujii, Mikiyasu Shirai, Shuji Inamori, Yoshiaki Takewa and Eisuke Tatsumi

Abstract— **Extracorporeal circulation (ECC) is indispensable for cardiac surgery. Since difficulty in clinical research keeps the knowledge insufficient, it is desirable to have a miniature ECC system for small animals. We aimed to establish a miniature ECC system and apply the system to the rat for investigating biochemical changes. The ECC system consisted of a membranous oxygenator (polypropylene, 0.03 m^2), tubing line (polyvinyl chloride) and roller pump. Priming volume of this system is only 15 ml. Rats were divided into the SHAM group and the ECC group. ECC pump flow was initiated and maintained at 70 ml/kg/min. We measured the serum cytokine levels of tumor necrosis factor-α, interleukin (IL)-6, and IL-10, and biochemical markers (lactate dehydrogenase, aspartate aminotransferase and alanine aminotransferase) before, 60, and 120 min after the initiation of ECC. In addition, we measured the wet-to-dry weight (W/D) ratio of the left lung tissues. During ECC, blood pressure and Hb were maintained around 80 mmHg and 10g/dl, the serum cytokine levels and biochemical markers were significantly elevated in the ECC group compared with the SHAM group. The W/D ratio increased significantly more in the ECC group compared with that in the SHAM group. These data suggest that ECC promotes organ damages and systemic inflammatory response. This rat ECC model is considered to be equivalent to the already established human ECC and useful for studying the mechanism of pathophysiological changes during artificial perfusion.**

I. Introduction

Extracorporeal circulation (ECC) is indispensable for cardiac surgery [1]. Despite the fact that ECC is traumatic to blood components and non-physiologic, its influence has not been fully elucidated. Since difficulty in clinical research and animal experiments keeps the knowledge insufficient, it is desirable to have a miniature ECC system for small animals to study the mechanism of pathophysiological changes in the circulation during ECC. Therefore, in this study, we measured the serum cytokine levels of tumor necrosis factor-α, interleukin (IL)-6, and IL-10, and biochemical markers (lactate dehydrogenase, aspartate aminotransferase and alanine aminotransferase) before, 60, and 120 min after the initiation of CPB. In addition, we measured the wet-to-dry weight (W/D) ratio of the left lung tissues.

Yutaka Fujii, Mikiyasu Shirai, Yoshiaki Takewa, and Eisuke Tatsumi are with the National Cerebral & Cardiovascular Center Research Institute, 5-7-1, Fujishiro-dai, Suita, Osaka, 565-8565, Japan (phone: 81-6-6833-5012; fax: 81-6-6835-5416; e-mail: yfujii@ ncvc.go.jp).

Shuji Inamori is with the Hiroshima International University, 555-36, Kurosegakuendai, Higashihiroshima, Hiroshima, 739-2631, Japan.

II. Materials and Methods

A. Animal

The study was approved by the National Cerebral and Cardiovascular Center Research Institute Animal Care and Use Committee, and all procedures met the National Institutes of Health guidelines for animal care.

Sprague-Dawley rats (male 400-450 g) were housed three per cage under a 12-h light-dark cycle with food and water available ad libitum.

B. Anesthesia, surgical preparation, and ECC

The animals were anesthetized with pentobarbital spdium (50 mg/kg body weight, intraperitoneal injection) and placed in the supine position with rectal thermocouple in place. Then, orotracheal intubation was performed using a 14G cannula (Insyte BD Medical, Sandy, UT, USA) and rats were ventilated with a respirator (Model SN-480-7, Shinano Seisakusho Co., Ltd, Tokyo, Japan). Ventilation was volume controlled at a frequency of 70/min, a tidal volume of 8-10 mL/kg body weight, and 40 % of inspired oxygen fraction. Rectal temperature was maintained at 36 ℃ throughout the experiment. Arterial blood pressure was monitored (Model 870, PowerLab system, AD Instruments, Castle Hill, NSW, Australia) via the femoral artery, which was cannulated with polyethylene tubing (SP-31 Natsume Seisakusho Co., Ltd, Tokyo, Japan). The left common carotid artery with a polyethylene tubing (SP-55 Natsume Seisakusho Co.) to serve as the arterial inflow cannula for the ECC circuit. 500 IU/kg heparin sodium was administered after placement of this cannula. A 16 G cannula (Insyte BD Medical) was advanced through the right external jugular vein into the right atrium and served as a conduit for venous outflow .

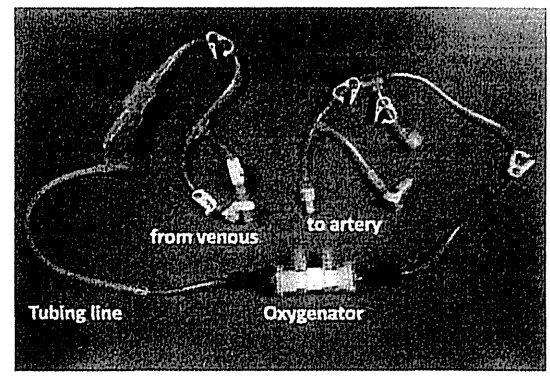

Figure 1. The small animal ECC system.

978-1-4244-7929-0/14/$26.00 ©2014 IEEE

The ECC circuit consisted of a membranous oxygenator (Senko Medical Co., Ltd, Osaka, Japan), tubing line (Senko Medical Co., Ltd) and roller pump (Micro tube pump MP-3 Tokyo Rikakikai Co., Ltd, Tokyo, Japan). The ECC circuit was primed by 14 ml of Ringer's solution bicarbonate and 1 ml (1000 IU) of heparin, total priming volume was 15 ml (Fig.1). Figure 2 shows the small animal ECC model schema.

C. *Experimental design*

The animals were divided into two groups: SHAM group (n=5), ECC group (n=7). The SHAM group received surgical preparation only without ECC. ECC pump flow was initiated and maintained at 70 mL/kg/min. Arterial pressure of carbon dioxide (PaO_2) and arterial pressure of oxygen (PaO_2) were maintained at 35-45 mmHg and 300-400 mmHg, respectively. Blood samples were collected at three defined time points, before ECC (pre-ECC), 60 min after initiation of ECC and 120 min after initiation of ECC (end-ECC).

To evaluate the inflammatory responses, TNF-α, IL-6, and IL-10 were measured (ELISA kit, R&D Systems, Minneapolis, MN, USA). The biochemical markers for evaluating organ damage (17), LDH, AST, and ALT were measured (DRI-CHE M 7000, Fujifilm, Kanagawa, Japan). Blood gases, pH, hemoglobin concentration, and electrolytes were also measured. Animals in which the hemoglobin level declined to less than 7 g/dL at any point were excluded from the study. All animals were sacrificed at the end of ECC by myocardial potassium injection and the left lung was harvested and divided into three parts. The superior third was used for the calculation of W/D ratio. The lung block was weighed before and after desiccation for 72 h in a drying oven at 70°C.

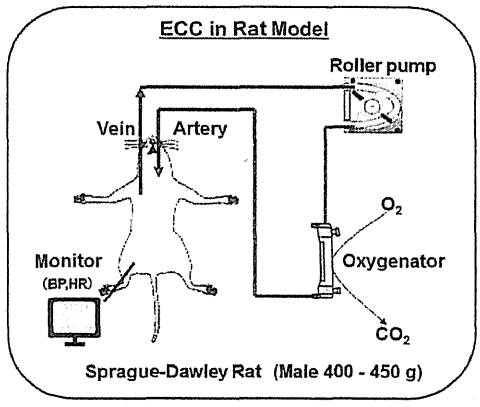

Figure 2. The small animal ECC model schema.

D. *Statistics*

All data are expressed as mean ± standard deviation. Comparison among groups was performed using analysis of variance. Fisher Protected Least Significant Difference post hoc test was used for subsequent comparison between groups at the same time. All statistical analyses were performed using Stat-View 5.0 (Abacus Concepts, Berkeley, CA, USA). Significance was set at $P < 0.05$.

III. RESULTS

Table 1 shows the changes in hemodynamic variables, Hb concentration and PaO_2 and $PaCO_2$ in SHAM and ECC groups during experiments. Mean arterial pressure (MAP) and Hb were significantly decreased during experiment in ECC groups.

TABLE I. HEMODYNAMIC VARIABLES, HB AND BLOOD GAS PARTIAL PRESSURES BEFORE AND DURING ECC

	Group	Pre-ECC	ECC 60 min	ECC 120 min
MAP (mmHg)	SHAM	103 ± 3	100 ± 5	104 ± 3
	ECC	105 ± 5	80 ± 3 †	76 ± 3 †
HR (beat/min)	SHAM	385 ± 15	385 ± 11	381 ± 7
	ECC	406 ± 9	358 ± 8	363 ± 8
PaO2 (mmHg)	SHAM	113 ± 8	106 ± 7	105 ± 6
	ECC	103 ± 8	464 ± 17 †	461 ± 16 †
PaCO2 (mmHg)	SHAM	38 ± 1	37 ± 1	40 ± 1
	ECC	40 ± 1	37 ± 1	36 ± 1
Hb (mg/dL)	SHAM	15.3 ± 1.0	15.2 ± 0.5	14.5 ± 0.4
	ECC	15.4 ± 0.2	10.1 ± 0.5 †	9.8 ± 0.4 †

Variables are expressed by mean ± standard error.
† $P < 0.05$ versus SHAM group at the same time.

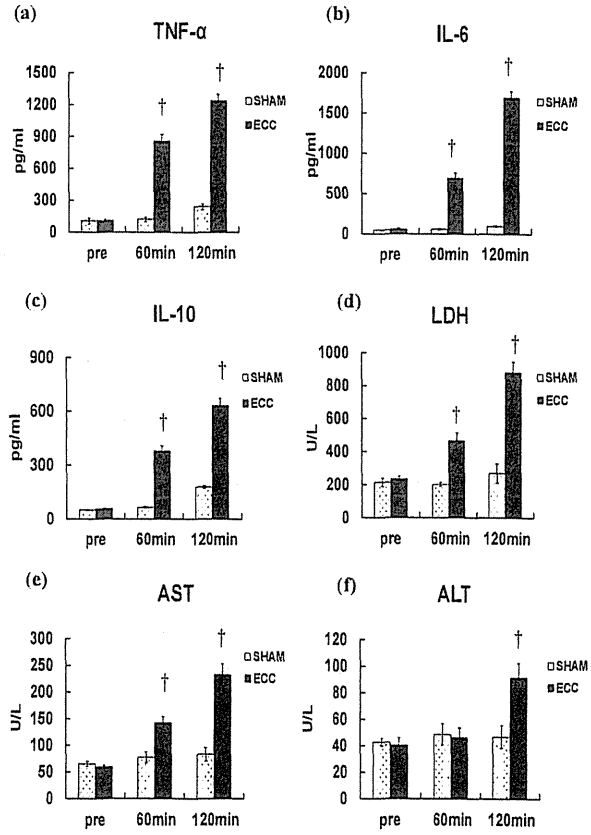

Figure 3. Serum TNF-α (a), IL-6 (b), IL-10 (c), LDH (d), AST (e), ALT(f).
† $P < 0.05$ versus SHAM group at the same time periods.

The PaO2 level was much higher in the ECC group (~460 mmHg) than in the SHAM group (~130 mmHg), while no statistical difference was found in the PaCO2 level between these groups.

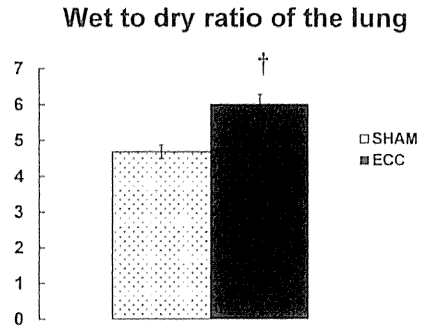

Figure 4. Wet to dry ratio of left lung at the end of ECC.
† P < 0.05versus SHAM group

Before ECC, the serum levels of inflammatory and biochemical markers were not statistically different among the SHAM and ECC groups. Serum inflammatory and biochemical markers remained unchanged during experiment periods in the SHAM group. In the ECC group, the cytokines and increased significantly, reaching a maximum (TNF-α : 1237 ± 62 pg/ml , IL-6 : 1695 ± 73 pg/ml, IL-10: 632 ± 40 pg/ml) at the end of ECC (Fig. 3a-c)

In the ECC group, the levels of biochemical markers significantly increased (LDH : 447±48 U/L, AST : 143±12 U/L, ALT : 46±7 U/L) 60 min after the ECC initiation and increased further (LDH : 882±62 U/L, AST : 233±20 U/L, ALT : 92±11 U/L) 120 min after the ECC initiation (Fig. 3d-e).

The ECC groups showed significantly higher W/D ratio than the SHAM group. (SHAM group : 4.68±0.08, ECC group : 6.01±0.10) (Fig.4).

IV. Discussion

In this study, our small animal ECC system was able to maintain adequate levels of blood gases ($PaCO_2$:35-45 mmHg, PaO_2: 300-400 mmHg), Hb (around the 10 g/dl level) and blood pressure (Mean arterial pressure more than 70 mmHg). Previous models have required high priming volumes to achieve acceptable hematocrit concentrations during the experiment. On the other hand, our model offers the advantage of a low priming volume not requiring transfusion in ECC group rats. Most previous research was performed in isolated heart models (e.g., Langendorff's method) [2]. By using our small animal ECC model, due to its minimal invasiveness and ease of recoverability, short- and long-term effects of ECC time, temperature (hypothermic condition), blood contact surface area and potentially also direct gene transfer on myocardial function and histological outcomes can be assessed better than in isolated heart models. While these models allow investigating the immediate effects of therapeutic interventions or different cardioplegia solutions, they preclude the assessment of long-term histological, biochemical, or functional outcomes. Survival studies using dogs or pigs [3,4] have been performed but are limited due to sample size and costs.

The present data showed that during the serum cytokine levels (TNF-α, IL-6 and IL-10) and biochemical markers (LDH, ALT, AST) were significantly elevated in the ECC group compared with the SHAM group, indicating that organ damage and a systemic inflammatory response occurred in our rat ECC model. During ECC, blood pressure and Hb were maintained around 80 mmHg and 10 g/dl, respectively. From these data, our rat ECC model is considered to be equivalent to the established human ECC, which is often associated with systemic inflammation and organ damage [5-7].

The significant systemic inflammatory responses occurred, reaching a maximum at the end of ECC. Additionally, the biochemical markers reflecting organ damages significantly increased 60 min after the ECC initiation and increased further 120 min after the ECC initiation. The significant increase in the W/D ratio which suggests pulmonary edema [8] is consistent with the previous clinical data [9]. From these data, our rat ECC model is considered to be equivalent to the established human ECC, which is often associated with systemic inflammation and organ damage [10].

It has been suggested that the factors responsible for the inflammatory response during ECC are blood contact with the surface of the extracorporeal circulation unit, endotoxemia, surgical trauma, ischemic reperfusion injury, and blood loss [11]. Many studies showed the walls of the ECC circuit activate white cells, platelets and the complement system. The increase in cytokines, such as interleukins and necrosis factor [12], aggravates the inflammatory response [13]. These complex interactions during ECC lead to further inflammation [13]. In our rat ECC models, the insufflation of hydrogen which selectively reduces the hydroxyl radical could decrease the levels of serum cytokines and biochemical markers, and the W/D ratio of the lung, suggesting that this radical contributes toward promoting the systemic inflammatory responses and organ damages during ECC [8].

Our previous study showed the selective reduction of hydroxyl radical with hydrogen gas attenuates both pro- and anti-inflammatory cytokines, suggesting that this radical acts to non-selectively increase these cytokines [8]. In addition, our new finding is that this increase in the W/D ratio was attenuated with hydrogen gas insufflation. Because ECC increases pulmonary vascular permeability, it is possible that hydrogen gas insufflation attenuates the injury of pulmonary vascular endothelium by scavenging reactive oxygen species and reducing the increase in vascular permeability during ECC. Although the detailed mechanism of the abovementioned anti-inflammatory effects of hydrogen gas insufflation was not elucidated in the previous study[8], this treatment may potentially serve as a novel clinical intervention in reducing the ECC-induced systemic inflammation. Solution of the inflammation mechanism during ECC require future research.

We have to study of due to its minimal invasiveness and ease of recoverability, short- and long-term effects of ECC time, temperature (hypothermic condition), blood contact surface area and potentially also direct gene transfer on myocardial function and histological outcomes. In addition, the model allows for the investigation of unique animal strains with varying susceptibility to myocardial injury depending on either their genetic background or disease (e.g., diabetes, old age, hypertension).

There are some limitations to this current model. Although our model closely resembles current clinical standards with respect to the ECC circuit, a number of potentially important differences to the clinical setting are present. Median sternotomy, direct surgery on the heart involving aortic cross-clamping, and cardiac arrest with the use of cardioplegia were not performed. Similarly, the absence of significant atheromatous disease and the complex comorbidities seen in patients undergoing coronary artery bypass graft surgery are limitations.

V. Conclusion

In this study, we developed a miniature ECC model and applied the system to the rat. In our rat ECC models, we demonstrated that adequate levels of blood gases and Hb, and blood pressure were maintained and that the systemic inflammatory response and organ damages including pulmonary edema were induced associated with the production of cytokines. We considered that our rat ECC model is equivalent to the established human ECC, which is often associated with systemic inflammation and organ damage. This miniature ECC model could be a very useful approach for studying the mechanism of pathophysiology during ECC and basic assessment of the ECC devices.

Acknowledgment

This work was supported by JSPS KAKENHI Grant Number 25871231 (Grant-in-Aid for Young Scientists B).

References

[1] Walker G, Liddell M, Davis C. Extracorporeal life support-state of the art. Paediatr Respir Rev 2003;4:147-52.

[2] Bopassa JC, Vandroux D, Ovize M, Ferrera R: Controlled reperfusion after hypothermic heart preservation inhibits mitochondrial permeability transition-pore opening and enhances functional recovery. Am J Physiol Heart Circ Physiol 2006, 291(5):H2265-71.

[3] Schmidt FE Jr., MacDonald MJ, Murphy CO, Brown WM 3rd, Gott JP, Guyton RA: Leukocyte depletion of blood cardioplegia attenuates reperfusion injury. Ann Thorac Surg 1996, 62(6):1691-6; discussion 1696-7.

[4] Fischer UM, Klass O, Stock U, Easo J, Geissler HJ, Fischer JH, Bloch W, Mehlhorn U: Cardioplegic arrest induces apoptosis signalpathway in myocardial endothelial cells and cardiac myocytes. Eur J Cardiothorac Surg 2003, 23(6):984-990.

[5] Laffey JG, Boylan JF, Cheng DC. The systemic inflammatory response to cardiac surgery: Implications for the anesthesiologist. Anesthesiology 2002;97:215-52.

[6] Boyle EM, Pohlman TH, Johnson MC, Verrier ED. Endothelial cell injury in cardiovascular surgery: the systemic inflammatory response. Ann Thorac Surg 1997;63: 277-84.

[7] Takahashi Y, Shibata T, Sasaki Y, Fujii H, Ikuta T, Bito Y, Nakahira A, Suehiro S. Impact of non-di-(2-ethylhexyl) phthalate cardiopulmonary bypass tubes on inflammatory cytokines and coagulation-fibrinolysis systems during cardiopulmonary bypass. J Artif Organs 2009;12:226-31.

[8] Fujii Y, Shirai M, Inamori S, Shimouchi A, Sonobe T, Tsuchimochi H, Pearson JT, Takewa Y, Tatsumi E, Taenaka Y.et al. Insufflation of Hydrogen Gas Restrains the Inflammatory Response of Cardiopulmonary Bypass in a Rat Model. Artif Organs 2013;37:136-41.

[9] Aebert H, Kirchner S, Keyser A, Birnbaum DE, Holler E, Andreesen R, Eissner G. et al. Endothelial apoptosis is induced by serum of patients after cardiopulmonary bypass. Eur J Cardiothorac Srug 2000;18:589-93.

[10] Boyle EM, Pohlman TH, Johnson MC, Verrier ED. Endothelial cell injury in cardiovascular surgery: the systemic inflammatory response. Ann Thorac Surg 1997;63: 277-84.

[11] Butler J, Rocker GM, Westaby S.Inflammatory response to cardiopulmonary bypass. Ann Thorac Surg 1993;55:552-9.

[12] Engelman RM, Rousou JA, Flack JE 3rd, Deaton DW, Kalfin R, Das DK. Influence of steroids on complement and cytokine generation after cardiopulmonary bypass. Ann Thorac Surg 1995;60:801-4.

[13] Cremer J, Martin M, Redl H, Bahrami S, Abraham C, Graeter T, Haverich A, Schlag G, Borst HG. Systemic inflammatory response syndrome after cardiac operations. Ann Thorac Surg 1996; 61:1714-20.

Application of a Search Algorithm Using Stochastic Behaviors to Autonomous Control of a Ventricular Assist Device

Kentaro Ohnuma, Hirohito Sumikura, Akihiko Homma, Tomonori Tsukiya, Toshihide Mizuno, Yoshiaki Takewa and Eisuke Tatsumi,

Abstract— **A ventricular assist device (VAD) is a device with mechanical pumps implanted adjacent to the patient's native heart to support the blood flow. Mechanical circulatory support using VADs has been an essential therapeutic tool for patients with severe heart failure waiting for a heart transplant in clinical site. Adaptive control of VADs that automatically adjust the pump output with changes in a patient state is one of the important approaches for enhanced therapeutic efficacy, prevention of complications and quality of life improvement. However adaptively controlling a VAD in the realistic situation would be difficult because it is necessary to model the whole including the VAD and the cardiovascular dynamics. To solve this problem, we propose an application of attractor selection algorithm using stochastic behavior to a VAD control system. In this study, we sought to investigate whether this proposed method can be used to adaptively control of a VAD in the simple case of a continuous flow VAD. The flow rate control algorithm was constructed on the basis of a stochastically searching algorithm as one example of application. The validity of the constructed control algorithm was examined in a mock circuit. As a result, in response to a low-flow state with the different causes, the flow rate of the pump reached a target value with self adaptive behavior without designing the detailed control rule based on the experience or the model of the control target.**

I. Introduction

A Ventricular Assist Device (VAD) is a device with mechanical pumps implanted adjacent to the patient's native heart to provide circulatory support (a left ventricular assist device, for example, pumps blood from the left ventricle to the aorta to assist blood flowing). Advanced hardware technology has enhanced the reliability of VAD long-term use, such as clinical application of implantable continuous flow VADs [1]. Accordingly, mechanical circulatory support using VADs has been an essential therapeutic tool for patients with severe heart failure waiting for a heart transplant [2]. On the other hand, considering about new treatment to recover cardiac function including destination therapy (DT) [3] or combination with myocardial regeneration therapy [4], there are many issues to solve, such as further device miniaturization, durability and antithrombogenicity improvements, circulation-control abnormality regardless of the improved treatment effects and stable blood flow, and various complications. To solve these issues, advanced software functionality such as VAD drive control may be equally important as hardware improvements. Many researchers have conducted studies on bypass flow control using cardiovascular mathematical models as well as continuous flow VAD optimization such as development of a function to change rotation speed via synchronization with the patient's heart rate [5-8]. Variations in rotation speed are expected to produce clinical effects including cardiac function recovery and complication prevention. Some devices have been already equipped with control functions to prevent outflow sucking and maintain bypass blood flow. At clinical sites, however, devices are usually used in a fixed rate or rotation number. Major reasons that the VAD automatic control functions are not used in practice are because of the difficulties in long-term stable measurement of biological information and modeling of complex circulatory systems controlled by the autonomic nerve or humoral factors. An algorithmic error consequent to an unexpected complex circulation behavior may cause dangerous device operation. These problems are likely to be solved when VADs are equipped with flexibly adaptive control like human body.

A recent physiological study has demonstrated that searching behaviors based on noise (or fluctuations) including muscle molecular level movement and heart rate variability play an important role in human adaptability [9-13]. Moreover, some researchers attempted to apply this mechanism to artificial object control such as robots or communication systems [14-17]. The objective of the present study was to realize ventricular assist devices which flexibly can response to unexpected changes. The mechanism of human adaptive behaviors was used to enable VADs to deal with the situations in which accurate modeling was considered difficult. Furthermore, this study was conducted to propose the application of a searching algorithm to VAD control using stochastic behaviors and to verify the beneficial effects on VAD control by this method according to the results of flow control. As the first step to investigate the benefits of this proposed method, continuous flow pumps, simple systems, were used to perform mock circulation tests.

II. Materials and Methods

A. Control Algorithm

Kashiwagi et al. proposed formula (1) called "attractor selection model" as a mathematical model to explain human sensing behaviors using noise [9].

Reserch supported by Grants-in-Aid for Scientific Research B (no. 24390308) and Grant-in-Aid for Challenging Exploratory Research (no. 25670563) from the Japan Society for the Promotion of Science and the Ministry of Education, Culture, Sports, Science and Technology of Japan.

K. Ohnuma, H. Sumikura, T. Tsukiya, T. Mizuno, Y. Takewa, E. Tatsumi are with the National Cerebral and Cardiovascular Center Research Institute, Suita, Osaka 565-8565, Japan (corresponding author to provide phone: +81-6-6833-5012; fax: +81-6-6835-5406; e-mail: ohnuma.kentaro@ri.ncvc.go.jp).

A. Homma is with Tokyo Denki University, Hatoyama, Saitama 350-0394, Japan.

978-1-4244-7929-0/14/$26.00 ©2014 IEEE

$$\dot{x} = -\nabla U(x) \cdot A + \eta \qquad (1)$$

In this formula, x, $U(x)$, A and η represent the system state, potential function (system dynamics), bias (an evaluation function indicating the goodness of fit for the system state) and noise (random variation), respectively. This model detects attractors via random walks; the inappropriate system state reduces Value A, and η becomes dominant.

To verify the benefits of this proposed method, attractor selection models were initially used to control and maintain blood flow on continuous flow pumps, comparatively simple systems. Continuous flow VADs mainly consist of a centrifugal pump or an axial flow pump. These pumps can adjust blood flow through changes in rotation speed on the internal impellers. Equation (2) is a general difference equation of formula (1).

$$x(t+1) = x(t) - A(t)\frac{dU(x(t))}{dx(t)} + \eta(t) \qquad (2)$$

To calculate the flow control on continuous flow pumps, the formula symbols were defined as follows: $x(t)$ = a control signal for rotation speed, $U(x)$ = a temporary target function (an approximate potential function with a turning point at $x(t)$ indicating the achievement of objective flow), A = an evaluation function to produce a $U(x)$-turning-point drawing effect, and η = noise. $U(x)$ was set with the Gaussian distribution function, and a parameter for the center of a turning point was defined as c as shown in a formula (3).

$$U(x) = a \times \exp\frac{-(x-c)^2}{2b} + d \qquad (3)$$

Constant a: Amplitude, b:Width of a temporary potential, c: Center of the potential, d: Offset

Value A tends to be high on a true $U(x)$ turning point; therefore, even when accurate $U(x)$ was not obtained because of the difficulty in modeling, c (the center of the $U(x)$ turning point) was updated to the side that had become high in the previous A by increasing or decreasing according to the Value A. This process allowed inaccurate $U(x)$ to draw to a potential neighborhood true value, and adaptive behaviors were expected accordingly. Value A is an important element which influences systems' behaviors. In this trial, we predicted behaviors to gain arbitrary objective blood flow, and experimentally set Formula (4) to provide a high value in case that the current flow is close to the desired value or the current difference from the objective flow is smaller than the previous difference.

$$A(t) = \frac{\exp\left(e \cdot \left(\left|Flow\_r(\tau-1) - Flow(\tau-1)\right| - \left|Flow\_r(\tau) - Flow(\tau)\right|\right)\right)}{\exp\left|f \cdot (Flow\_r(\tau) - Flow(\tau))\right|} \qquad (4)$$

e, f: Constant, $Flow$: Mean flow rate, $Flow\_r$: objective flow rate, τ: observation time of $Flow$

After η was defined as Gaussian noise, a bias was added to the median value according to the increase or decrease in the previous A, in order to improve the search efficiency.

B. Mock Circulation Test

To evaluate behaviors based on the implemented algorithm, control testing on a closed loop for mock circulation was performed using a prototype model of a developing axial flow pump [18]. The axial flow pump used had a structure to rotate the impeller in the brushless direct current motor, and this was the same as a general continuous flow VAD. In addition, the axial flow pump had a mechanism to support the rotor with the internal impeller through fluid dynamic bearing (Figure 1). This pump was connected to a soft reservoir via the inflow and outflow PVC tube (inner diameter: 1/2 in., length: 1 m, respectively), and the supply side on the pump was equipped with the function of circulatory resistance to generate the pump head (Figure 2). The motor of this pump was operated by a widely-used motor driver which was able to change rotation speed via external signals. The working fluid was 37 wt% glycerol-water solution at 27 degrees Celsius.

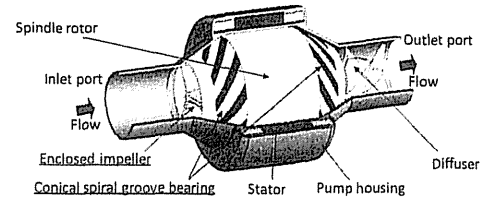

Figure 1. Structural drawing of a prototype axial flow pump under development used in the mock circulation test.

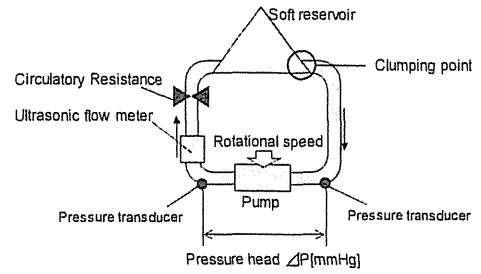

(a) Mock circulation loop

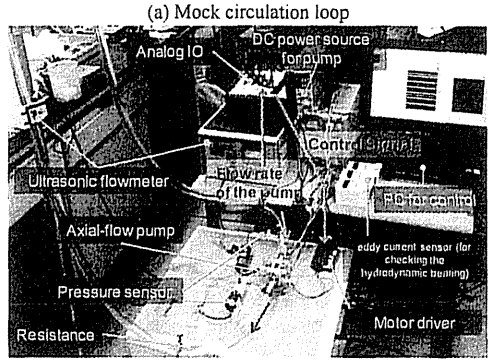

(b) Experimental setup and control system

Figure 2. Schematic diagrams of mock circulation test (measurement items, ⊿P [mmHg]: Pressure sensors, Flow rate [L/min]: Ultrasonic flowmeter, Control signal: x [V], Parameter of the control: $dU(x), A, c, \eta$).

The rotation speed control was designed to provide a feedback when any flow signal calculated by the ultrasonic flow meter (T106, Transonic Systems Inc.) is input into the PC and subsequently to output an implementation signal calculated by the proposed algorithm. A pressure sensor (PA-500, Nidec Copal Electronics Corp.) was used to determine the pump inflow- and outflow-side pressure, pump flow measured by the ultrasonic flow meter, and rotation speed control signals and also to record the control parameters ($\Delta U(x)$, A, c, and η). The sampling and parameter updating

cycle were set to 100 Hz and 1 sec, respectively. As the target pump used had a levitated dynamic bearing structure, the algorithm was designed assuming that the actual rotation speed corresponding to rotation speed control signals were known. The rotation speed received from the control signals was set in the range of 7000-12000 rpm so that the bearing was able to maintain stable levitation.

A random rotation number was set to run the pump operation testing. Subsequently, the target flow was set to 5 L/min to begin this control algorithm. Initially, the circulatory resistance was changed to examine the basic behavior, and we observed the variations in the flow, rotation speed, control signal, and other control parameters accordingly. Secondly, inflow sucking (extreme negative pressure on inflow side because of a flow obstruction) was generated on the pump assuming that the environment was unexpectedly changed to evaluate the behavior. The sucking was generated by the tube on the inflow side and the soft reservoir connection part from the outside (Figure 2. (a)), which were unclamped soon after a sucking condition was satisfied (Before this procedure, we conducted a stationary operation to confirm that the negative pressures caused by sucking were not automatically released at the event of full sucking). Similarly, the changes in the pump behaviors were observed.

III. Results

Figure 3 lists the results of the circulatory resistance changes. In this test, our proposed method was used to control the blood flow of an axial flow pump to maintain an arbitrary target flow. The objective flow of 5 L/min was achieved when this control was added to pump operation by the steady rotation speed of 4.5 L/min. Subsequently, when the circulatory resistance was reduced, the following changes were obtained: 1. the pump flow increased, 2. η became

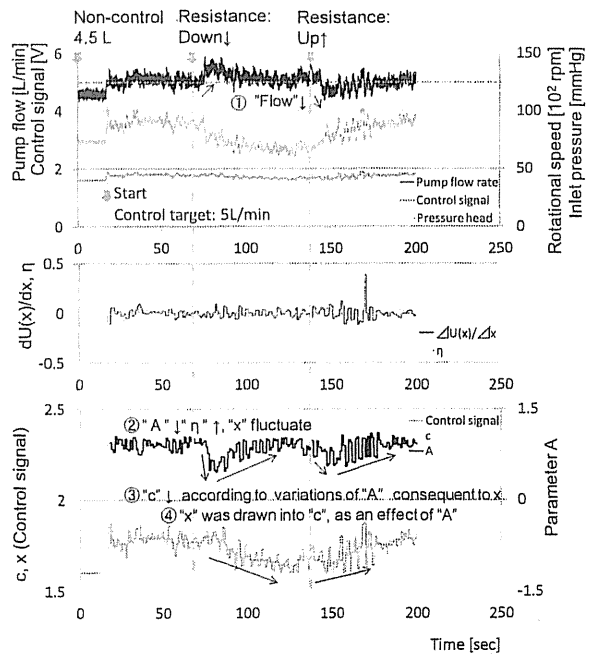

Figure 3. The behavior of the pump to changes of the circulatory resistance

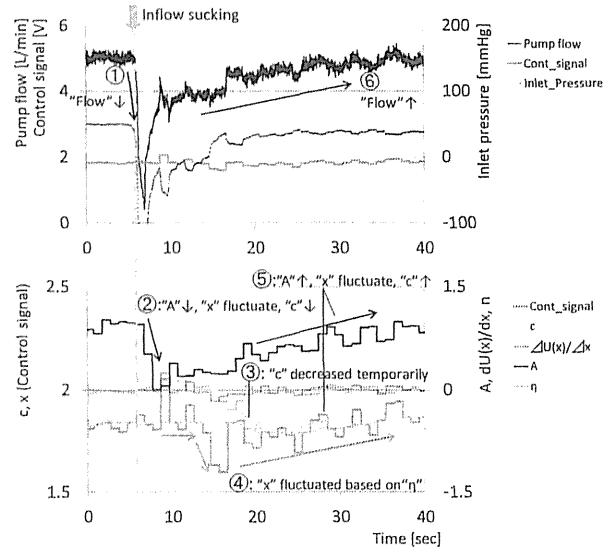

Figure 4. One example of the adaptive behavior on inflow obstruction (unexpected disturbance).

dominant because of a decrease in A and this changed x, 3. c was updated along with the change of A consequent to x, and finally 4. x was drawn into c, the center of $U(x)$, as an effect of A. Accordingly, the flow achieved the desired value again. We observed that the flow achieved to the target value when the circulatory resistance increased further after it had reached the initial value.

Furthermore, one case of behaviors in inflow sucking was listed in Figure 4. According to the result, 1. the flow decreased because of inflow sucking, 2. a decrease in A allowed η to be dominant and this changed A consequent to the variation in x, 3. c temporally decreased, 4. the negative pressure on the inflow side was released after c was drawn into c, 5. A increased because of recovery of the flow and c also increased tentatively, and 6. the flow reached the target value again. Similarly, the target flow was achieved throughout 10-time attempts, even though the results varied widely (24.1±16.4 sec) because of the sucking degrees and noise effects.

IV. Discussion

As tasks of this trial, a rotation speed increase and temporary decrease were required when the blood flow decreased because of a circulatory resistance increase and sucking, respectively. Flow maintenance and sucking release could be realized by other means; however, in this method, different behaviors were required for the same flow-decrease phenomenon. Therefore, the self-adjusting behaviors observed in this study should be significantly useful to develop more flexibly adaptive ventricular assist device control, because those results were obtained without the provision of any additional sensor for sucking detection as well as the design of behavioral rules based on some models or experiences. Furthermore, this study demonstrated that the method was able to cope with dynamic objects and first or low-frequency events regardless of the disadvantages of accuracy and speed. However more detailed behaviors should be investigated for severe conditions on the circulation.

At clinical sites in which continuous flow VADs are used, sucking on the ventricle insert site of an inflow cannula is acknowledged as a problem; thus, this method which can solve sucking automatically is likely useful. In this trial, the probe of the ultrasonic flow meter used was connected to the outflow tube to determine the pump flow. A general continuous flow VAD has a function to estimate flow from current or other values. Nevertheless, it is difficult to provide accurate data in situations such as sucking. Some ultrasonic flow meter probes are able to be used with blood vessel prostheses for VAD blood supply; however, long-term stable measurements of flow are likely difficult in implantable continuous flow VAD patients. As many researchers have pointed out, development of long-term stable flow measurements is a major task with respect to implantable continuous flow VADs [19-22], and this is also essential for this flow control algorithm. Meanwhile, testing under pulsatile pressure must be performed to investigate the behaviors of this algorithm, in consideration of blood inflow from the patient's native heart. With the exception of c, the parameters, constant a, b, d of $U(x)$, control cycle, e & f corresponding to the weight of A, and bias of noise η were set by trial and error approach. To establish the evaluation and design methods to optimize these parameters is another task.

In this trial, the control to maintain flow was executed using the feedbacks of pump flow measurements. This algorithm is able to be applied not only to flow control but also other processes. A and x can be respectively independent in regard to this method. Therefore, if further technical developments enable macroscopic index sensing such as judging on VAD patients' circulation conditions or comfort, pumps using this method may cope with sensing situations easily even if the relationship between the indices of evaluation function A and pump flow is not clear. In addition, combinatory use of this proposed method with currently-used VAD control methods may enable stable VAD systems to behave without algorithm errors, because this method is able to help to adapt other control algorithms to the human body.

V. Conclusion

In this study, we proposed a searching control method and performed axial flow pump flow control using a mock circulation loop. As a result, the control to maintain the target flow determined at the design phase was successfully achieved. When sucking, an unexpected event, occurred, the target flow was recovered via the self-adjusting behavior without designing the detailed control rule based on the experience or the model of the control target.

Accordingly, this method was proved useful with respect to autonomous VAD control.

References

[1] Slaughter MS, Pagani FD, Rogers JG, *et al.* "Clinical management of continuous-flow left ventricular assist devices in advanced heart failure", J Heart Lung Transplant, 29(45), S1-39, 2010

[2] Garrick C Stewart, Michael M Givertz, "Mechanical circulatory support for advanced heart failure: Patients and technology in evolution", Circulation, 125(10), pp.1304-15, 2012

[3] Kyo S, Minami T, Nishimura T, *et al.* "New era for therapeutic strategy for heart failure: Destination therapy by left ventricular assist device", Journal of Cardiology, 59(2), pp. 101-109, 2012

[4] Sawa Y, "Current status of myocardial regeneration therapy", Gen Thorac Cardiovasc Surg. 2013 Jan;61(1):17-23. doi: 10.1007/s11748-012-0153-9. Epub 2012 Nov 7

[5] AlOmari AH, Savkin AV, Stevens M, Mason DG, Timms DL, Salamonsen RF, Lovell NH, "Developments in control systems for rotary left ventricular assist devices for heart failure patients: a review", Physiol. Meas. 34 R1–R27, 2013

[6] Wu Y, "Adaptive physiological speed/flow control of rotary blood pumps in permanent implantation using intrinsic pump parameters", ASAIO J. , 55(4), pp. 335-9, 2009

[7] Ando M, Nishimura T, Takewa Y, Yamazaki K, Kyo S, Ono M, Tsukiya T, Mizuno T, Taenaka Y, Tatsumi E, "Electrocardiogram-synchronized rotational speed change mode in rotary pumps could improve pulsatility", Artif. Organs, 35(10), pp. 941-947, 2011

[8] Umeki A, Nishimura T, Ando M, Takewa Y, Yamazaki K, Kyo S, Ono M, Tsukiya T, Mizuno T, Taenaka Y, Tatsumi E, "Alteration of LV end-diastolic volume by controlling the power of the continuous-flow LVAD, so it is synchronized with cardiac beat: development of a native heart load control system (NHLCS), J Artif. Organs, 15(2), pp. 128-133, 2012

[9] A. Kashiwagi, I. Urabe, K. Kaneko, T. Yomo, "Adaptive response of a gene network to environmental changes by fitness-induced attractor selection", PLoS ONE, 1: e49, 2006

[10] M. Nishikawa, H. Takagi, T. shibata, A. H. Iwane, T. Yanagida, "Fluctuation Analysis of Mechanochemical Coupling Depending on the Type of Biomolecular Motors", Phys. Rev. Lett. 101, 128103, 2008

[11] M. Iwaki, A. H. Iwane, T. Shimokawa, R. Cooke, T. Yanagida, "Brownian search-and-catch mechanism for myosin-VI steps", Nat. Chem. Biol 5(6), pp. 403-405, 2009

[12] T. Kuusela, T. Shepherd, J. Hietarinta, "Stochastic model for heart-rate fluctuations", Phys Rev E67, 061904, 2003

[13] T. Kuusela, "Stochastic heart-rate model can reveal pathologic cardiac dynamics", Phys Rev E69, 031916, 2004

[14] A. Sugahara, Y. Nakamura, I. Fukuyori, Y. Matsumoto, and H. Ishiguro, Generating circular motion of a human-like robotic arm using attractor selection model. Journal of robotics and mechatronics 22(3), pp. 315-321, 2010

[15] Y. Koizumi, T. Miyamura, S. Arakawa, E. Oki, K. Shiomoto, and M. Murata, Adaptive virtual network topology control based on attractor selection, IEEE/OSA Journal of Lightwave Technology 28(11), pp. 1720-1731, 2010

[16] Y. Minami, Y. Koizumi, S. Arakawa, T. Miyamura, K. Shimoto, M. Murata, "Benefits of Virtual Network Topology Control based on Attractor Selection in WDM Networks", International Journal on Advances in Internet Technology, 4(1- 2), pp. 79-88, 2011

[17] S.G. Nurzaman, Y. Matsumoto, Y. Nakamura, S. Koizumi, and H. Ishiguro, ""Yuragi" based adaptive mobile robot search with and without gradient sensing: from bacterial chemotaxis to Levy walk", Advanced Robotics, 25(16), pp.2019—2037, 2011

[18] Sumikura H, Fukunaga K, Funakubo A, Fukui Y, "Verification of enclosed-impeller for an axial flow blood pump by using computational fluid dynamics analysis", Journal of Life Support Engineering, 20, pp. 9-16, 2008, in japanease

[19] Funakubo A, Ahmed S, Sakuma I and Fukui Y, "Flow rate and pressure head estimation in a centrifugal blood pump", Artif. Organs, 26, pp. 985-990, 2002

[20] Tsukiya T, Taenaka Y, Nishinaka T, *et. al.*, "Application of indirect flow rate measurement using motor driving signals to a centrifugal blood pump with an integrated motor", Artif. Organs, 25, pp. 692-696, 2001

[21] Ogawa D *et. a.l.* , "Indirect flow rate estimation of the NEDO PI Gyro pump for chronic BVAD experiments", ASAIO J. , 52, pp. 266–271, 2006

[22] Kitamura T, Matsushima Y, *et. al.*, "Physical model-based indirect measurements of blood pressure and flow using a centrifugal pump", Artif. Organs, 24, pp. 589-593, 2000

J Artif Organs (2014) 17:135–141
DOI 10.1007/s10047-014-0757-1

ORIGINAL ARTICLE

Artificial Heart (Basic)

Novel control system to prevent right ventricular failure induced by rotary blood pump

Mamoru Arakawa · Takashi Nishimura · Yoshiaki Takewa · Akihide Umeki · Masahiko Ando · Yuichiro Kishimoto · Yutaka Fujii · Shunei Kyo · Hideo Adachi · Eisuke Tatsumi

Received: 5 September 2013 / Accepted: 20 January 2014 / Published online: 7 February 2014

Abstract Right ventricular (RV) failure is a potentially fatal complication after treatment with a left ventricular assist device (LVAD). Ventricular septal shift caused by such devices is an important factor in the progress of RV dysfunction. We developed a control system for a rotary blood pump that can change rotational speed (RS) in synchrony with the cardiac cycle. We postulated that decreasing systolic RS using this system would alter ventricular septal movement and thus prevent RV failure. We implanted the EVAHEART ventricular assist device into seven adult goats weighing 54.1 ± 2.1 kg and induced acute bi-ventricular dysfunction by coronary embolization. Left and RV pressure was monitored, and ventricular septal movement was echocardiographically determined. We evaluated circuit-clamp mode as the control condition, as well as continuous and counter-pulse modes, both with full bypass. As a result, a leftward ventricular septal shift occurred in continuous and counter-pulse modes. The septal shift was corrected as a result of decreased RS during the systolic phase in counter-pulse mode. RV fractional area change improved in counter-pulse (59.0 ± 4.6 %) compared with continuous (44.7 ± 4.0 %) mode. In conclusion, decreased RS delivered during the systolic phase using the counter-pulse mode of our new system holds promise for the clinical correction of ventricular septal shift resulting from a LVAD and might confer a benefit upon RV function.

Keywords Artificial organs · Rotary blood pump · LVAD · Right ventricular failure

M. Arakawa (✉) · Y. Takewa · Y. Kishimoto · Y. Fujii · E. Tatsumi
Department of Artificial Organs, National Cerebral and Cardiovascular Center Research Institute, 5-7-1 Fujishiro-dai, Suita, Osaka 565-8565, Japan
e-mail: a_mamoru@mbn.nifty.com

M. Arakawa · H. Adachi
Department of Cardiovascular Surgery, Saitama Medical Center, Jichi Medical University, Saitama, Japan

T. Nishimura (✉) · S. Kyo
Department of Cardiac Surgery, Tokyo Metropolitan Geriatric Hospital, 35-2 Sakae-cho, Itabashi-ku, Tokyo, 173-0015, Japan
e-mail: takashin-tyk@umin.ac.jp

T. Nishimura · A. Umeki · M. Ando
Department of Cardiothoracic Surgery, University of Tokyo, Tokyo, Japan

Introduction

Left ventricular assist device (LVAD) therapy is considered effective for treating patients with end-stage heart failure, either as a bridge to transplantation [1] or as destination therapy [2]. Continuous-flow LVADs are now widely applied, owing to a decrease in complications and improved prognoses compared with pulsatile LVADs [3]. However, differences in physiological effects between continuous-flow and pulsatile LVADs remain controversial [4–6], especially those involving right ventricular (RV) function [7]. The probability of RV failure does not seem to differ between pulsatile and continuous-flow LVADs [7], but differences in the physiological effects between these devices remain unclear.

RV failure is a life-threatening complication for patients treated with an LVAD [8]. Physiologically, an LVAD is thought to have both beneficial and adverse effects on the right ventricle [9, 10]. One reason for the beneficial effect on RV function is that LVAD unloading leads to a decrease in RV afterload through a decrease in pulmonary artery